Proceedings of the American Control Conference
Philadelphia, Pennsylvania • June 1998

Impedance Control with Varying Stiffness for Parallel-Link Manipulators

Jong H. Park and Hyun C. Cho
Hanyang University, Seoul, 133-791, Korea
(e-mail: jongpark@email.hanyang.ac.kr)

Abstract

This paper proposes a new impedance control algorithm based on a variable stiffness-matrix, for parallel-link manipulators without the measurement of the tip position. It assumes that only the link lengths and velocities as well as the contact force at the tip are measured, and that the motion range is small around an operating point so that the nonlinear dynamics can be linearized. One of the key ideas is to change the stiffness matrix of the impedance model in order to compensate dynamics model parameter errors.

In simulations, it is shown that despite the simplicity of the algorithm, its performance is similar to that of the control law based on the nonlinear dynamics with the correct parameters estimates, and that it is robust to estimation errors of some parameters such as the platform mass and the leg masses.

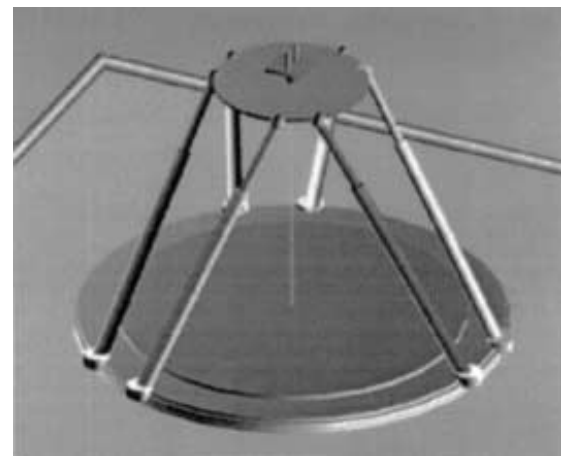

Figure 1: The parallel-link manipulator used in this paper.

1. Introduction

In many robotic tasks, robot manipulators interact with their environments. Excessive contact force between the manipulator and the environment should be prevented. One method to limit excessive force is the force control, which simply limits the magnitude of the external force. For more elaborated tasks such as one that requres force control in one direction and position control in another direction, hybrid position/force control has been proposed. For general interaction with the environment, more powerful impedance control is used.

Impedance control, proposed by Hogan [1], adjusts the impedance of the manipulator, which is defined as $Z(s) = F(s)/V(s)$ where $F(s)$ denotes force and $V(s)$ denotes velocity in the Laplace transform; and is determined typically by an inertia, a damper, and a spring. The desired impedance of the manipulator depends on the task that the manipulator performs. Since the task is in general expressed in the world coordinates, the desired impedance characteristics should be also expressed in the world coordinates.

A 6-dof parallel-link manipulator in general consists of a fixed base, a moving plate and 6 links between them (See Fig. 1). One end of a link is connected to the base and the other to the plate. The length of each link is controlled by an actuator. Characteristics of parallel-link manipulators are quite different from those of serial manipulators. Due to their parallel-link structures, they are very stiff and have large load capacity. Thus, they have been used as machine tools such as underground excavation instrument [2], milling machines [3] as well as positioning devices for radars. However, their small work space is a drawback.

From the control point of view, one of the most important characteristics different from serial link manipulators is that solving the forward kinematics is difficult. This means that it is difficult to compute the parallel link manipulator tip position by the measurement of link lengths. Since the tip position should be known in order to obtain a desirable characteristics of the manipulator impedance, this makes the implementaion of impedance control for parallel-link manipulators very difficult.

In order to resolve the difficulty in solving the forward kinematics, a few methods have been suggested such as estimating the tip position iteratively using numerical methods [4], approximating the forward kinematics with neural networks [5], using a passive serial links to measure directly the joint angles, and then measure the tip position with sensors [2].

In this paper, we propose an alternative method of implementing the impedance control for parallel-link manipulators. This method requires only the measurement of link lengths, their velocity and the force exerted by the environment, and is based on the linearization of the nonlinear dynamics under the assumption of small manipulator motions. It also changes stiffness matrix of the impedance model so that the effects of the parameter modeling errors can be nullified. This method is compared in simulations with two other impedance control

0-7803-4530-4/98 $10.00 © 1998 AACC

methods based on the nonlinear and linearized dynamics.

Section 2 describes the dynamics of the parallel-link manipulator and its linearized version. Section 3 explains the proposed impedance control algorithm for parallel-link manipulators, as well as two other control algorithms, for the purpose of performance comparisons. Simulation results of the impedance control algorithms and comparisons of their performance are shown in Section 4, which is followed by conclusions in Section 5.

2. Manipulator Dynamics

It is known that dynamic equations of parallel-link manipulators are easier to drive in the Cartesian space than in the joint space [6]. Some forms of dynamic equations such as one suggested by Lebret [6] are similar to those for serial-link manipulators but very complex to be used in computing the control input. In this paper, the dynamic equation suggested by Ji [7] for parallel-link manipulators is used.

$$M(x)\ddot{x} + C(x,\dot{x}) = D(x)\tau + F_e \tag{1}$$

where $x \in \mathbb{R}^6$ denotes the tip position (and orientation), $\tau \in \mathbb{R}^6$ denotes the force generated at the joints, and $F_e \in \mathbb{R}^6$ is the external force (and moment).

Deriving a control law from the nonlinear dynamics requires the measurement of the manipulator tip position. However, measuring the tip position is more difficult than measuring the lengths of the parallel links. One way to avoid the measurement of the tip position is to use the linearized dynamics expressed in the joint space.

Let's define a function f for the linearization.

$$f(x,\dot{x},\ddot{x},\tau,F_e) = M(x)\ddot{x} + C(x,\dot{x}) - D(x)\tau - F_e \tag{2}$$

Linearizing f about an operating point $(x_0,\dot{x}_0)$ under the assumption that it is partially differentiable,

$$\bar{M}\delta\ddot{x} + \bar{C}\delta\dot{x} + \bar{G}\delta x = \bar{D}\delta\tau + F_e \tag{3}$$

where

$$\bar{M} = \left.\frac{\partial f}{\partial \ddot{x}}\right|_0 = M(x_0) \qquad \bar{C} = \left.\frac{\partial f}{\partial \dot{x}}\right|_0$$
$$\bar{D} = -\left.\frac{\partial f}{\partial \tau}\right|_0 = D(x_0) \qquad \bar{G} = \left.\frac{\partial f}{\partial x}\right|_0.$$

$$\delta x = x - x_0$$

and

$$\delta\tau = \tau - \tau_0.$$

τ_0 is the torque required to maintain the motion x_0, $\dot{x}_0$ and $\ddot{x}_0$. In most applications, $\dot{x}_0 = \ddot{x}_0 = 0$. If this is the case, $\tau_0 = D^{-1}(x_0)C(x_0,0)$.

3. Impedance Control

3.1. Impedance Model

Impedance model is a relationship between the manipulator tip position and its contact force. Impedance is choisen according to robot tasks, which are often expressed in the world coordinates. Thus, the desired impedance models are in general expressed in the world coordinates. Suppose that the following impedance model in the world coordinates is desired.

$$M_x\delta\ddot{x} + B_x\delta\dot{x} + K_x\delta x = \delta F_e \tag{4}$$

where δx is the difference between the actual position x and the desired position x_d that is assumed to be identical to x_0, i.e., $\delta x = x - x_d = x - x_0$; M_x, B_x, and K_x are the inertia matrix, damping matrix and stiffness matrix of the desired impedance, respectively; and $\delta F_e = F_e - F_d$ where F_e is the external force and F_d is the desired external force.

In order to use the impedance model expressed in the world coordinates, the meaurement of the manipulator tip position is required. In order to avoid such measurement, the desired impedance in the world coordinates should be transformed into the desired impedance in the joint space. The transformation can done by assuming again that manipulator motions are small in size around a reference point.

From the kinematics and statics, the following relations can be derived.

$$\delta\ell = J(x_0)\delta x \tag{5a}$$
$$\delta\dot{\ell} = J(x_0)\delta\dot{x} \tag{5b}$$
$$\delta\ddot{\ell} = J(x_0)\delta\ddot{x} \tag{5c}$$

and

$$\delta F_e = J^T(x_0)\delta\tau_e \tag{6}$$

where $J(\cdot)$ is the manipulator Jacobian.

By substituting Eq. 5 and Eq. 6 into Eq. 4, the impedance model in the joint space can be obtained.

$$M_\ell\delta\ddot{\ell} + B_\ell\delta\dot{\ell} + K_\ell\delta\ell = \delta\tau_e \tag{7}$$

where

$$M_\ell = J^{-T}(x_0)M_xJ^{-1}(x_0) \tag{8a}$$
$$B_\ell = J^{-T}(x_0)B_xJ^{-1}(x_0) \tag{8b}$$
$$K_\ell = J^{-T}(x_0)K_xJ^{-1}(x_0) \tag{8c}$$

$$\delta\ell = \ell - \ell_0$$

and

$$\delta\tau_e = \tau_e - \tau_d$$

where τ_e is the torque reflected by the external force F_e so that

$$F_e = J^T(x_0)\tau_e,$$

and the desired torque τ_d is also defined such that

$$F_d = J^T(x_0)\tau_d.$$

3.2. Impedance Control Using Nonlinear Dynamics and Impedance Model

If the meaurement of the manipulator tip position can be measured, the control law to achieve the impedance model of Eq. 4 can be obtained easily. Assuming that M_x is nonsingular, acceleration $\ddot{x}$ can be removed by using Eq. 4 and Eq. 1.

$$\tau = D(x)^{-1}\Big(M(x)\Big(M_x^{-1}(\delta F_e - B_x\delta\dot{x} - K_x\delta x) + \ddot{x}_0\Big) + C(x,\dot{x}) - F_e\Big) \quad (9)$$

Note that F_e could have been removed instead of $\ddot{x}$ by using Eq. 4 and Eq. 1. This would not rquire the measurement of the external force F_e; however, the control law would include a term of $\ddot{x}$, which is very difficult to measure due to noises. Impedance-controlled systems without the measurement of the contact force are known to be slow in response.

3.3. Impedance Control Using Linear Dynamics and Impedance Model

The control law in Eq. 9 cannot be used if the measurement of the tip position is not available and if only the link positions and velocities as well as the external force are measured. One way to implement the impedance control is to use the dynamics and the impedance model expressed in the joint space. Thus, by using the linearized dynamics (Eq. 3) and linearized impedance model (Eq. 7) in the joint space, a linear control law can be obtained.

$$\tau = K_v\delta\dot{\ell} + K_p\delta\ell + K_f\delta F_e - \bar{D}^{-1}F_e + \tau_0 \quad (10)$$

where

$$K_v = \bar{D}^{-1}(\bar{C} - \bar{M}M_x^{-1}B_x)J^{-1}(x_0)$$
$$K_p = \bar{D}^{-1}(\bar{G} - \bar{M}M_x^{-1}K_x)J^{-1}(x_0)$$
$$K_f = \bar{D}^{-1}\bar{M}M_x^{-1}$$

Equation 10 needs the measurement of the link positions and velocities, and the external force only. All the coefficients in Eq. 10 are constant, and thus can be precomputed.

3.4. Impedance Control Using Varying Stiffness and Linear Dynamics

The previous two control laws perform well as long as there's no or little uncertainty in the manipulator parameters. However, their performance deteriorates with increases of uncertainty. Especially, the control law based on the linearization exhibits unsatisfying behaviors with large errors in the parameter estimates.

In order to increase the robustness of the system to the uncertainty of the system parameters, it is suggested to change the stiffness matrix of the impedance model.

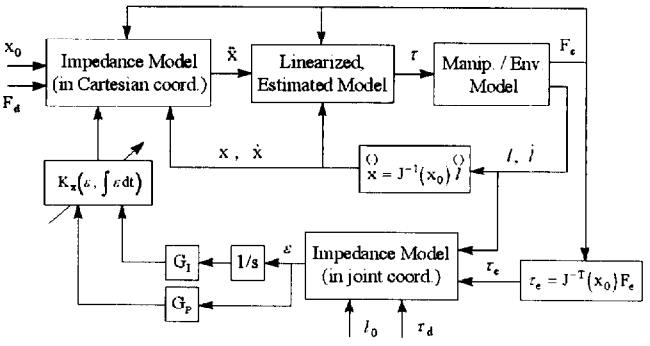

Figure 2: Overall system block diagram including the varying stiffness controller and the manipulator/environment.

Table 1: Manipulator parameters

Parameter	Actual Value	Estimate
radius of the base	0.6 (m)	0.6 (m)
radius of the platform	0.6 (m)	0.6 (m)
mass of the platform	20. (kg)	10.0 (kg)
mass of an upper leg	2.0 (kg)	1.5 (kg)
mass of a lower leg	6.0 (kg)	5.0 (kg)

First, let's define an impedance error vector $e \in \mathbb{R}^6$.

$$e = M_\ell\delta\ddot{\ell} + B_\ell\delta\dot{\ell} + K_\ell\delta\ell - \delta\tau_e \quad (11)$$

If the manipulator behaves precisely according to the impedance model, then $e = 0$.

Kazerooni et al. [8] note that the manipulator response under impedance control is very much dictated by the stiffness matrix of the impedance model when it is subject to an external low-frequency force. Thus, we suggest to change the impedance stiffness matrix in Eq. 10 depending on the impedance error and its integration over time, i.e.,

$$\tilde{K}_x = K_{x0}\cdot\left(I + G_P E + G_I\int E\,dt\right) \quad (12)$$

where K_{x0} is the stiffness matrix of the desired impedance; G_P and G_I are diagonal gain matrices; and $E = \mathrm{diag}(e_1, e_2, \ldots, e_6)$ is an impedance error matrix.

Then, the control law becomes

$$\tau = K_v\delta\dot{\ell} + \tilde{K}_p\delta\ell + K_f\delta F_e - \bar{D}^{-1}F_e + \tau_0 \quad (13)$$

where

$$\tilde{K}_p = \bar{D}^{-1}(\bar{G} - \bar{M}M_x^{-1}\tilde{K}_x)J^{-1}(x_0) \quad (14)$$

The overall system block diagram including the varying stiffness impedance controller, the manipulator and the environment is shown in Fig. 2.

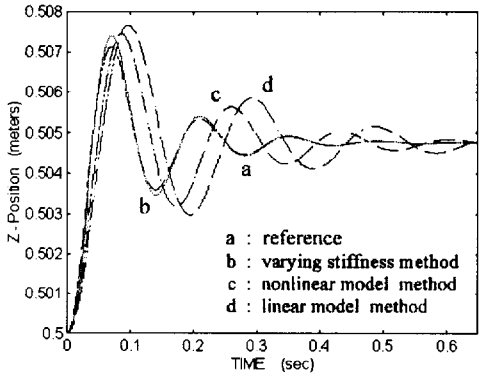

Figure 3: Motion responses of the control laws when the manipulator tip is in contact with the environment.

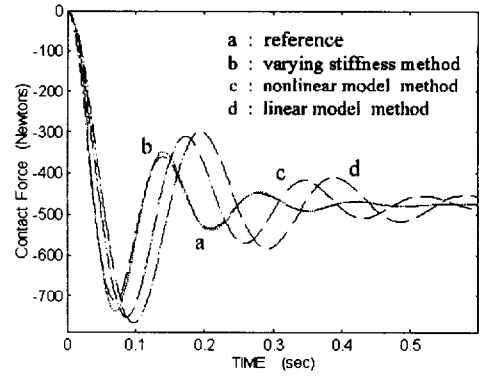

Figure 4: Contact force responses of the control laws when the desired force is 500 N.

4. Simulation

Performace of the control laws are compared in a series of simulations of a 6-dof parallel-link manipulator. The important manipulator parameters are shown in Table 1. Actual parameters are used in the simulation of the manipulator dynamics and the estimates are used in computing the control laws for the effects of parametric uncertainty. Only the uncertainty in the masses are considered. In the simulation, it is assumed that the desired position is x_0.

The manipulator tip is initially just in contact with the environment located at $[0 \quad 0 \quad 0.5 \quad 0 \quad 0 \quad 0]^T$ with respect to the center of the base. Each control law of Eq. 9, Eq. 10, and Eq. 13 are used to have the desired z-directional external force $F_{d,z} = 500$ [N].

The parameters of the desired impedance model are selected as $M_x = \text{diag}(50, 50, \ldots, 50)$ [kg; Nms^2], $B_x = \text{diag}(1000, 1000, \ldots, 1000)$ [Ns/m; Nms], and $K_x = \text{diag}(5000, 5000, \ldots, 5000)$ [N/m; Nm]. The external environment is modeled as a spring-damper system with $B_e = \text{diag}(50, 50, \ldots, 50)$ [Ns/m; Nms] and $K_e = \text{diag}(10^5, 10^5, \ldots, 10^5)$ [N/m; Nm].

The response of the manipulator system for each control law is shown in Fig. 3. The "reference" denotes the case when the nonlinear control law of Eq. 9 implemented with *the exact estimates* of the parameters. The figure shows that the varying stiffness control of Eq. 13 performs very similarly to the reference despite the errors in the parameter estimates, and is superior to the nonlinear control law of Eq. 9 with the identical errors in the parameter estimates. Fig. 4 shows force responses of the control laws. The varying stiffness control performs again very closely to the "reference" and is superior to the other algorithms with errors in the parameter estimates, especially in terms of overshoots and duration of transient periods.

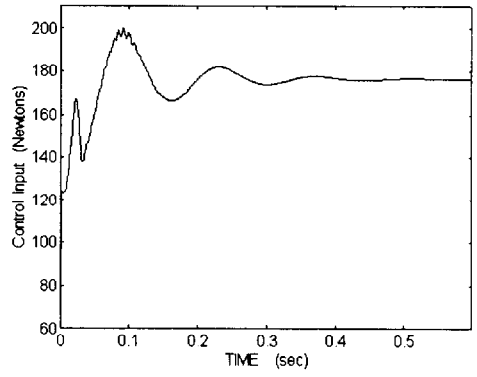

Figure 5: Control input (i.e., force) generated by one of the legs when varying stiffness control is used.

Figure 5 shows the control input, i.e., force generated at one of the legs when the varying stiffness control is used. Large force is generated in the beginning of the motion when the large acceleration is required. The varying stiffness also becomes very large at this moment. Figure 6 indicates that the varying stiffness initially becomes very large and negative for some time. Such large negative stiffness in the beginning results in generating larger force than the one computed based on

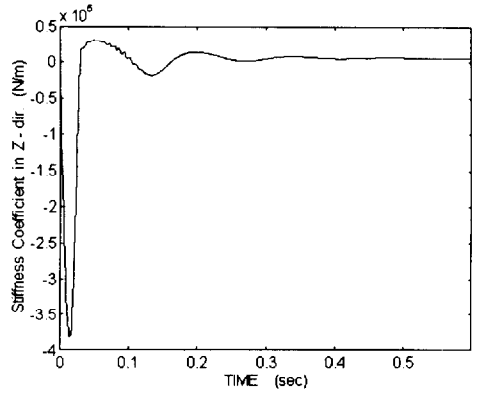

Figure 6: The stiffness changes when varying stiffness control is used.

the impedance model. This large force is needed to compensate the underestimated masses of the manipulator.

Even though the control performance is robust, it is noted that the size of gain G_P influences the manipulator performace. Simulations results show that the manipulator performs well when the gain is set to be inversly proportional to the desired force. Gain G_I is to remove the steady state impedance error.

5. Conclusions

An impedance control algorithm based on the linearized dynamics and the varying stiffness of the impedance model is suggested. In simulations, it is shown that this control algorithm is superior to the impedance control algorithm based on the nonlinear dynamics when parameter estimation errors exist. More work is to be done in selecting the optimal impedance error gains of the controller depending on manipulator tasks.

References

[1] N. Hogan, "Impedance control: An approach to manipulation, Parts I–III," *Journal of Dynamic Systems, Measurement, and Control*, vol. 107, pp. 1–24, 1985.

[2] T. Arai *et al.*, "Development of a parallel link manipulator," *Fifth International Conference on Advanced Robotics*, pp. 839–844, 1991.

[3] S. M. Satya, P. M. Ferreira, and M. W. Spong, "Hybrid control of a planar 3-dof parallel manipulator for machining operations," *Transactions of NAMRI/SME*, vol. 23, pp. 273–280, 1995.

[4] K. Cleary and T. Brooks, "Kinematic analysis of a novel 6-dof parallel manipulator," *Proceedings of the IEEE International Conference on Robotics and Automation*, pp. 708–713, 1993.

[5] Z. Geng and L. Haynes, "Neural network solution for the forward kinematics problem of a Stewart platform," *Proceedings of the IEEE International Conference on Robotics and Automation*, pp. 2650–2655, 1991.

[6] G. Lebret, K. Liu, and F. L. Lewis, "Dynamic analysis and control of a Stewart platform manipulator," *Journal of Robotic Systems*, pp. 629–655, 1993.

[7] Z. Ji, "Study of the effect of leg inertia in Stewart platform," *Proceedings of the IEEE International Conference on Robotics and Automation*, pp. 121–126, 1993.

[8] H. Kazerooni, T. B. Sheridan, and P. K. Houpt, "Robust compliant motion for manipulators, part i: The fundamental concepts of compliant motion," *Proceedings of the IEEE International Conference on Robotics and Automation*, 1986.